DOI:10.1021/jf903309s

JOURNAL OF AGRICULTURAL AND FOOD CHEMISTRY
ARTICLE

Interaction of Water with Three Granular Biopesticide Formulations

Margaret E. Lyn,*,† Dan Burnett,§ Armando R. Garcia,§ and Ron Gray§

†Application and Production Technology and Biological Control of Pests Research Units, Agricultural Research Service, U.S. Department of Agriculture, Stoneville, Mississippi 38776 and §Surface Measurement Systems Ltd., Suite 1, 2125 28th Street S.W., Allentown, Pennsylvania 18103

Two obstacles for biopesticide commercialization, long shelf life and reliable efficacy, are both affected by moisture availability. Three biopesticide delivery systems, TRE-G, PEC-G, and PESTA, were analyzed by dynamic vapor sorption analysis. The objective was to investigate the moisture sorption profile of each system in air at 25 °C and a relative humidity (RH) ranging from 0 to 90%. The formulations sorbed up to 12.7% moisture. In rehydrating from 0.00 to 90% RH, TRE-G and PEC-G were ≥63% and ≥58% faster than Pesta, respectively. In losing moisture from 90 to 0.00% RH, Pesta was 3.4 and 2.3 times slower than TRE-G and PEC-G, respectively. The GAB model was inadequate for describing moisture sorption, but the Young and Nelson model showed good correlation ($r > 0.990$) for all three formulations. Moisture distribution for all formulations was obtained. The implications of the findings as they relate to shelf life and dew period requirements of biopesticides are discussed.

KEYWORDS: Water sorption isotherms; dynamic vapor sorption (DVS); moisture sorption kinetics; biological control; biopesticide formulations; biopesticide development

INTRODUCTION

Despite the efforts of more than 15 years of intercontinental research devoted to various aspects of discovering useful pathogens and developing viable propagules as biopesticides, numerous research gaps remain for these technologies that are to be applied seasonally like synthetic pesticides. There are some bioinsecticides and biofungicides available commercially, but only a few bioherbicides have been registered globally to date (*1*). As noted by Jones and Burges (*2*), formulations of beneficial microorganisms to control different agricultural pests share common strengths and technological weaknesses. Development is often hampered by complex, interrelated biotechnological challenges relating to production, stabilization, and stimulation of the biologically active material (*3*). After extensive evaluations to identify a microbial pesticide, obstacles that are likely to be encountered later in a development process include the development of formulations that (a) are compatible with existing application technologies, (b) protect biological actives from infrared/heat or ultraviolet radiation in the field, (c) ensure viability remains high or relatively unchanged after storage and transport under ambient conditions, (d) ensure prolonged contact between microbial actives and target weeds, (e) ensure moisture availability in the field, and (f) are cost-effective.

Water activity is a parameter that regulates microbial activity (*4*). The importance of this parameter in relation to field efficacy of particular bioherbicides (*5*,*6*) and bioinsecticides (*7*) is known. Moreover, technological strategies to improve field efficacy, in particular for bioherbicides, have not been reliable to date and could lead to other complications including phytotoxicity or require innovative application technologies (*8*). These measures have been through the inclusion of humectants or through development/application of emulsion-type formulations (*6*, *9*, *10*) to prolong moisture availability. The importance in relation to shelf life, herein related to conidial longevity, has also been investigated (*7*, *11*−*14*). Whereas high water activities may stimulate growth, unwanted growth or germination during storage can be controlled by both reducing and maintaining the water activity at or near an ideally low level (*4*, *11*, *12*). Although these studies confirm the need to dehydrate microbial formulations below a particular water activity threshold, there are drawbacks associated with many of these studies as they achieve static and discrete water activities via saturated salt solutions. Salt solution studies cannot easily address other practical issues of concern such as whether there is an optimal low water activity level that may be microbial and/or formulation dependent. They also cannot easily address how the formulation would respond to incremental changes in relative humidity (RH) of the air in which the formulation is being stored or applied. Furthermore, water activity levels and thresholds are limited to the selection of saturated salts used. Sorption isotherms generated from studies using salt solutions show poor continuity of data or limited water activity range (*11*, *15*). Also, inconsistent responses from conidia of *Beauveria bassiana* stored over saturated salt solutions and hermetic storage have indicated that storage over salt solutions may be problematic for biopesticide research (*16*).

An alternative to the use of salt solutions is an automatic water sorption analyzer that continuously monitors moisture uptake or loss in response to changes in the relative humidity of the air around the sample. Although time-consuming to determine

*Author to whom correspondence should be addressed (e-mail Margaret.Lyn@ars.usda.gov).

 Published on Web 01/08/2010

experimentally even with a sorption analyzer, sorption isotherms are important in the prediction of shelf life, selection of storage conditions and packaging materials, and determination of other relevant research and development data and decisions (*17*). To our knowledge, there has not been any investigation aimed at probing the dynamics of water uptake of biopesticide formulations in relation to changes in either ambient temperature or humidity that did not involve the use salt solutions.

Water activity (A_w) indicates the amount of so-called "free" or "unbound" water in a system and is mathematically equivalent to the decimal of relative humidity as shown in eq **1**.

$$A_w = P/P_0 = \mathrm{RH}/100 \quad (1)$$

Here, P is the partial pressure of water above the sample, P_0 is the vapor pressure of pure water at the sample temperature, and RH is the equilibrium relative humidity (%) of the air around the sample. In solid formulations, water can be present in different states. These states as classified in the literature may be bound, free, capillary, mobile, nonsolvent, and/or unfreezable (*18*). At least 77 different models are available to describe the states of water within food and food products (*19*, *20*). Some are strictly theoretical in origin, whereas others are empirically or semi-empirically derived. These models are utilized in industries, for example, pharmaceutical, food, and cosmetics, where product properties are affected by water content and activity. Several models have been proposed because no single model has been successful in describing water interaction with all types of products and over the entire water activity range from 0 to 1. However, a few models have become more popular than others in use. The Guggenheim−Anderson−de Boer (GAB) equation (*21*), the Brunauer−Emmett−Teller (BET) equation (*22*), and the Young and Nelson (Y&N) equation (*23*, *24*) are all examples of widely used models.

In the present study, the moisture sorption isotherms of three clay-based biopesticide delivery systems denoted TRE-G, Pesta, and PEC-G were analyzed using a dynamic vapor sorption analyzer and were fitted with the GAB and Young and Nelson models. The main objective is to evaluate the usefulness of the dynamic vapor sorption technology to biopesticide research and development. The aim is to investigate the water uptake/loss behavior of the three biopesticide formulations over the 0−90% relative humidity range at 25.0 °C. Microscope images were collected in situ over the range of humidity conditions to detect any visible, moisture-induced changes in the formulations. The implications of differences in sorption behavior and any visible changes will be discussed along with the potential significance of these studies in developing microbial-based biopesticides.

MATERIALS AND METHODS

Sorption Analysis. Dynamic gravimetric vapor sorption (DVS) is a well-established method for the determination of vapor sorption isotherms (*25*, *26*). The DVS-1 instrument (Surface Measurement Systems, London, U.K.) used for these studies measures the uptake and loss of vapor gravimetrically using a Cahn D200 (Thermo Scientific, Waltham MA) recording ultramicrobalance with a mass resolution of ±0.1 μg. The high mass resolution and baseline stability allow the instrument to measure the adsorption and desorption of very small amounts of probe molecule. The vapor partial pressure around the sample is controlled by mixing saturated and dry carrier gas streams using electronic mass flow controllers. The temperature is maintained constant ±0.1 °C by enclosing the entire system in a temperature-controlled enclosure.

Preparation of Formulations. Satintone 5HB, a calcined kaolin clay, was provided by Englehard Corp. (Iselin, NJ) for use as a carrier in the TRE-G and PEC-G granule formulations. Sodium carboxymethylcellulose (Nilyn XL 90), provided by FMC Corp. (Philadelphia, PA), was used as a binder in addition to trehalose (Cargill, Inc., Minneapolis, MN) for the TRE-G formulation. However, only pectin (Sigma Aldrich) was used as a binder in PEC-G. The composition of the dry ingredients in the TRE-G formulation was 76% Satintone 5HB, 4% sodium carboxymethylcellulose, and 20% trehalose (*27*). For PEC-G, the composition was 85% Satintone 5HB and 15% pectin and is an alternative formulation to TRE-G.

Dry ingredients were mixed until visually homogeneous in a food processor before mixing in approximately 100% w/w (of dry ingredients) 0.1% (w/v) peptone solution to the TRE-G mixture or 87% w/w deionized water of the dry mixture for PEC-G. Both of the TRE-G and PEC-G mixtures were extruded in a pan granulator (LCI Corp., Charlotte, NC) equipped with a 1.2 mm die and dried respectively in a vacuum oven and a fluid bed dryer to a water activity of approximately 0.30. The Pesta sample, >2 years old, was already available. It was prepared by a twin-screw extruder as described by Daigle et al. (*28*) and was composed of 40% semolina, 26.7% kaolin, and 33.3% rice flour on a dry matter basis. The samples were stored at 4 °C before use.

Sample Preparation for Sorption Analysis. Previously stored formulations at 4 °C were transferred to a desiccator at ∼25 °C until they were ready to be run in the DVS instrument. For the vapor sorption experiments, each formulation was loaded into the DVS sample pan and immediately placed into the DVS with a stream of dry (<0.1% relative humidity) air. The sample was analyzed on a DVS-1 automated sorption analyzer at the desired temperature (25.0 °C) with a sample size between 17 and 30 mg. The sample size was sufficient due to the high sensitivity (0.1 μg) and balance baseline stability of the microbalance used in the DVS instrument.

Sorption Measurements. For each vapor sorption/desorption isotherm experiment, the sample was first dried under a continuous flow of dry air (relative humidity < 0.1%) to establish the dry mass, M_0. The sample was then exposed to the following partial pressure profile: 0−90% RH in 10% RH steps under a linear air flow speed of 22.1 cm/min. The RH was then decreased in a similar manner to accomplish a full sorption/desorption cycle. A second complete sorption/desorption cycle was collected to detect any irreversible humidity cycling effects. After the experiment was completed, the sample was inspected visually to detect if any changes occurred during the DVS experiment.

During the experiment, the instrument was run in dm/dt mode (mass variation over time variation) to determine when mass equilibrium is reached after each humidity increase or decrease. A fixed dm/dt value of 0.001% min^{-1} was selected as the criterion for equilibrium for all partial pressure segments. This criterion permits the DVS software to automatically determine when equilibrium has been reached and complete a relative humidity step. When the rate of change of mass falls below this threshold over a determined period of time, the relative humidity set point will proceed to the next programmed level. A maximum stage time of 360 min and a minimum stage time of 15 min were selected for these experiments.

At the end of each relative humidity step, digital color images were collected in situ via the video microscopy accessory (Surface Measurement Systems) to optically detect any moisture-induced structural changes. The microscope sits below the sample and captures images at the end of each RH step. The camera captures digital color images at 100× magnification.

For data analysis, two different isotherm models that offer extended water activity range of application were selected to model the experimentally measured sorption isotherms. The GAB and Y&N models were used to fit the moisture sorption isotherms for all three formulations. The data were analyzed by multiple regression analysis that was done using the DVS Isotherm Analysis Suite (v. 2.1.1) software package by Surface Measurement Systems.

Mathematical Models. *GAB Equation.* The GAB model is an extension of the BET model. It is a kinetics model based on the formation of multimolecular layers and condensation and is recommended by the European Project Group COST 90 on physical properties of food for the characterization of water sorption of food materials due to the relatively wider A_w range (0.05−0.9) in comparison to the BET model (0.05−0.5) (*29*).

The GAB equation can be written in many forms. The most common is

$$W = \frac{W_m C K A_w}{(1 - K A_w)[1 + (C - 1) K A_w]} \quad (2)$$

where W is the moisture content of the sample on a dry mass basis at a

water activity of A_w. The three remaining terms, W_m, C, and K, are sorption parameters that are characteristics of the formulation. The W_m term is the GAB monolayer capacity, which indicates moisture content corresponding to the monomolecular layer on the entire free surface of the sample, whereas C and K are so-called "energy" constants related to the heat of sorption for the monolayer and the layers above the monolayer or the intermediate layers, respectively. According to the model, water molecules in the first monolayer interact more strongly with the sample than molecules in the intermediate layers.

Y&N Model. Young and Nelson (*23*, *24*) hypothesized that water interacting with a sample is subjected to two types of forces. In addition to surface binding forces accounted for in the GAB model, Young and Nelson hypothesized that diffusional forces were also present and that this force could become dominant when multimolecular layers of water were present. It was further hypothesized that as the amount of surface water increased, diffusional forces would increase and ultimately exceed binding surface forces to enable movement of water into the sample. In addition to providing insight into the distribution of water in a sample, the model also provides an explanation for the observation of a hysteresis. According to the model, when the relative humidity of the environment is reduced, movement of water from within the sample occurs after the molecular layers have been removed. This movement, also driven by diffusional forces, is caused by moisture concentration gradients within and around the sample.

The experimental sorption and desorption data can be fitted with one of the following equations:

$$M_S = A(\theta + \alpha) + B\varphi \quad (3)$$

$$M_D = A(\theta + \alpha) + B\theta RH_{max} \quad (4)$$

M_S and M_D are equilibrium moisture contents for the respective cycle at each relative humidity, and RH_{max} is the maximum relative humidity that the sample is exposed to. The A and B terms are characteristic of the formulation and are defined as

$$A = \frac{\rho_w V_{ads}}{D} \quad (5)$$

$$B = \frac{\rho_w V_{abs}}{D} \quad (6)$$

where ρ_w is the density of water at the experimental temperature, D is the sample dry weight, and V_{ads} and V_{abs} are, respectively, the volumes of adsorbed and absorbed water. The Greek terms θ, α, and φ in eqs **3** and **4** are related to an E term through the mathematical expressions

$$\theta = \frac{RH}{RH + (1 - RH)E} \quad (7)$$

$$\alpha = -\frac{ERH}{E - (E-1)RH} + \frac{E^2}{(E-1)} \ln\left[\frac{E - (E-1)RH}{E}\right] - (E+1)\ln(1 - RH) \quad (8)$$

$$\varphi = \theta RH \quad (9)$$

where the E term is given as

$$E = e^{-\left[\frac{q_1 - q_L}{k_B T}\right]} \quad (10)$$

In eq **10**, q_1 (J/mol) is the heat of adsorption of water bound to the surface of the sample, q_L (J/mol) is the heat of condensation of water molecules, k_B is Boltzmann's constant (1.38×10^{-23} J/K), and T (K) is the absolute temperature at which the experiment is carried out. The experimental data must be fitted to determine the values of A, B, and E for each sample because V_{ads}, V_{abs}, and q_1 are unknown parameters.

RESULTS AND DISCUSSION

Morphological Changes. Water interactions with pharmaceutical or food formulations are well-known. Besides influencing microbial activity, water facilitates chemical reactions by either acting as a solvent or as a reactant, especially in hydrolysis reactions. In food products, moisture levels measured as water activity affect chemical reactions such as lipid autoxidation, vitamin degradation and Maillard reactions in addition to chemical properties such as the stability of proteins and activity of enzymes by enabling conformational changes. Because most biopesticide formulations are composed of common food ingredients and materials, similar conclusions regarding moisture-induced changes within a biopesticide could be expected. Microscope images were collected in situ over the 0−90% RH range to detect any visible, moisture-induced changes in TRE-G, Pesta, and PEC-G.

Representative images for TRE-G, Pesta, and PEC-G are displayed in **Figure 1**, panels **A**−**C**, respectively, at 0% RH sorption and 90% RH sorption. The video images did not reveal any optically discernible water sorption induced morphological changes over the 0−90% RH range. The images taken at 0, 10, 50, and 90% RH for each formulation are nearly indistinguishable (data not shown). TRE-G, PEC-G, and Pesta all remain structurally intact in environments up to 90% RH. Furthermore, desiccation after exposure to 90% RH did not appear to induce any macroscopic changes to these formulations (data not shown). Although no major morphological changes are apparent, there may be a slight degree of swelling as the humidity is increased, which could be attributed to water interaction with carbohydrates present in each formulation, in particular to polysaccharides (*30*). Visible inspection of the formulations after the experiment was completed indicated that no changes were observable by the naked eye.

Moisture Sorption and Desorption Isotherms. The relationship between equilibrium moisture content and water activity of a sample at a constant temperature is a moisture sorption isotherm. This may be presented graphically or as an equation. When the sorption and desorption isotherms differ over all or part of the water activity range, a so-called hysteresis occurs. Herein, the criterion used for equilibrium was a constant dm/dt value of 0.001% min^{-1}. Furthermore, the samples were allowed a maximum stage time of 360 min and a minimum stage time of 15 min at each relative humidity. By imposing these conditions on the definition of equilibrium, no equilibrium is reached when either the absolute value of $dm/dt > 0.001\%$ min^{-1} or when a sample requires >360 min to equilibrate. In these studies, $|dm/dt|$ exceeded 0.001% min^{-1} at 0% between cycles for TRE-G (−0.00190% min^{-1}) and at 70% (0.00121% min^{-1}) and 90% (0.00124% min^{-1}) (absorption, cycle I), 10% (−0.00101% min^{-1}) (desorption, cycle I), 0% (−0.00148% min^{-1}) between cycles, and 10% (−0.00102% min^{-1}) (desorption, cycle II) for Pesta. In other words, TRE-G and Pesta require >360 min to reach equilibrium at particular relative humidities. Therefore, the presented isotherms are not associated with absolute equilibrium but instead are based on the criterion for equilibrium as described above.

The water vapor isotherm plots for the three formulations are shown in **Figure 2**, panels **A** (TRE-G), **B** (Pesta), and **C** (PEC-G). The equilibrium sample weight at 0% RH was used as the reference for all subsequent sample weights. The isotherm plots shown in **Figure 2** display the percent change in mass (referenced from the dry mass, M_0) versus the actual percent partial pressure of water vapor (see eq **1**). The red and green traces follow the sorption portion of the isotherm, whereas the blue and pink traces follow the desorption portion of the isotherm during the first and second cycles, respectively.

All three formulations sorb significant amounts of water. For instance, at 90% RH, the TRE-G, Pesta, and PEC-G

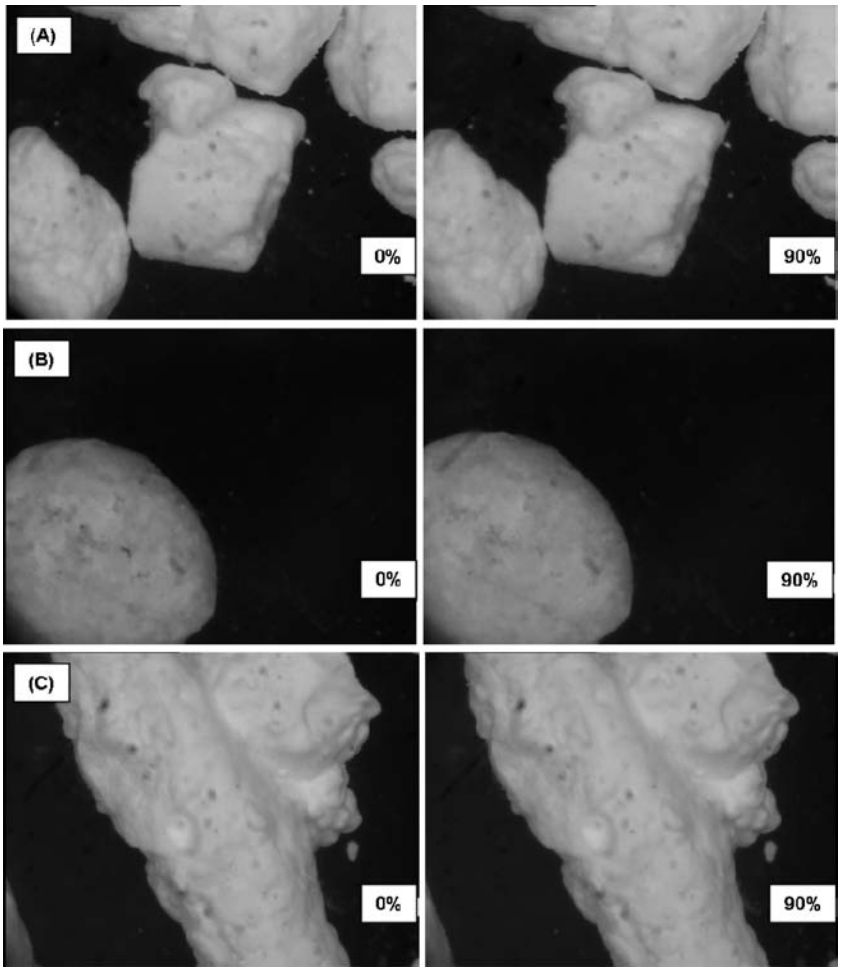

Figure 1. Video images collected of TRE-G (**A**), Pesta (**B**), and PEC-G (**C**) during the first sorption cycle at 0 and 90% RH sorption stage.

formulations sorbed up to 5.0% (**Figure 2A**), 12.7% (**Figure 2B**), and 5.6% (**Figure 2C**) moisture (based on dry weight), respectively. All three formulations are nonporous materials. These relatively large changes in mass suggest the presence of a bulk absorption mechanism or an absorption process coupled to adsorption in contrast to moisture uptake solely by adsorption. This is most evident for the Pesta and PEC-G formulations. The presence of a bulk moisture absorption mechanism is also supported by other moisture sorption properties. First, all three formulations exhibit relatively slow sorption kinetics (discussed below). Second, the three formulations show significant hysteresis (**Figures 2**) across a wide range of humidities (discussed below). Collectively, these results indicate a dominant mechanism of bulk absorption for all three formulations.

Although the formulations sorb significant amounts of water and appear to do so by a similar mechanism, there are notable differences in sorption properties. In particular, the degree of hysteresis and water uptake capacity were quite different among formulations. **Figure 2** shows the comparison between the sorption (red and blue traces) and desorption (green and pink traces) isotherms for the three formulations. The formulations are distinguishable by their hysteresis. Notable differences between each formulation are the hysteresis loop shape and the degree of hysteresis over the A_w range. The degree of hysteresis obeys the trend TRE-G < PEC-G < Pesta for both cycles 1 and 2 (**Table 1**). Whereas a maximum in hysteresis is reached at a low A_w or ~0.10 for TRE-G, the maximum occurs in the mid to low A_w range (i.e., 0.30−0.60) for Pesta and in the mid to high range (i.e., 0.50−0.70) for PEC-G. The variations in hysteresis across these formulations are not surprising because the type of main constituent material(s) is known to affect the hysteresis (*31*). Similarly, hysteresis loop shapes are also governed by the type of materials in the sample in addition to the sample temperature. Hysteresis can be grouped into three food categories: high-sugar, high-protein, and high-starch foods. In the former, there is an absence of hysteresis above 0.65, whereas the total hysteresis may be large in contrast to the second case, where a moderate hysteresis begins at 0.85. In the latter case, a large hysteresis loop is generally observed with a maximum in hysteresis at ~0.70 (*31*). A trend that is consistent with a high-sugar food is observed for TRE-G, whereas Pesta and PEC-G exhibit hysteresis comparable to high-starch foods. This may be attributed to the relatively high percent composition of trehalose in TRE-G and the starch materials in Pesta and PEC-G. Differences in hysteresis maximum between these pseudofood materials and pure food materials may be attributed to the clay constituent in TRE-G, Pesta, and PEC-G.

Whereas a small hysteresis loop suggests surface layer sorption, a large hysteresis loop is indicative of bulk absorption uptake coupled with a diffusion-limited desorption mechanism. The degree of hysteresis observed for the three formulations (**Table 1**) indicates that water desorption from the bulk is most likely diffusion-limited or that the diffusion rates of water from within the bulk to the surface and from the surface to the surrounding atmosphere are comparatively slower than that of the overall sorption process.

TRE-G, Pesta, and PEC-G are also distinguishable by their water uptake capacity. The absolute uptakes among the three

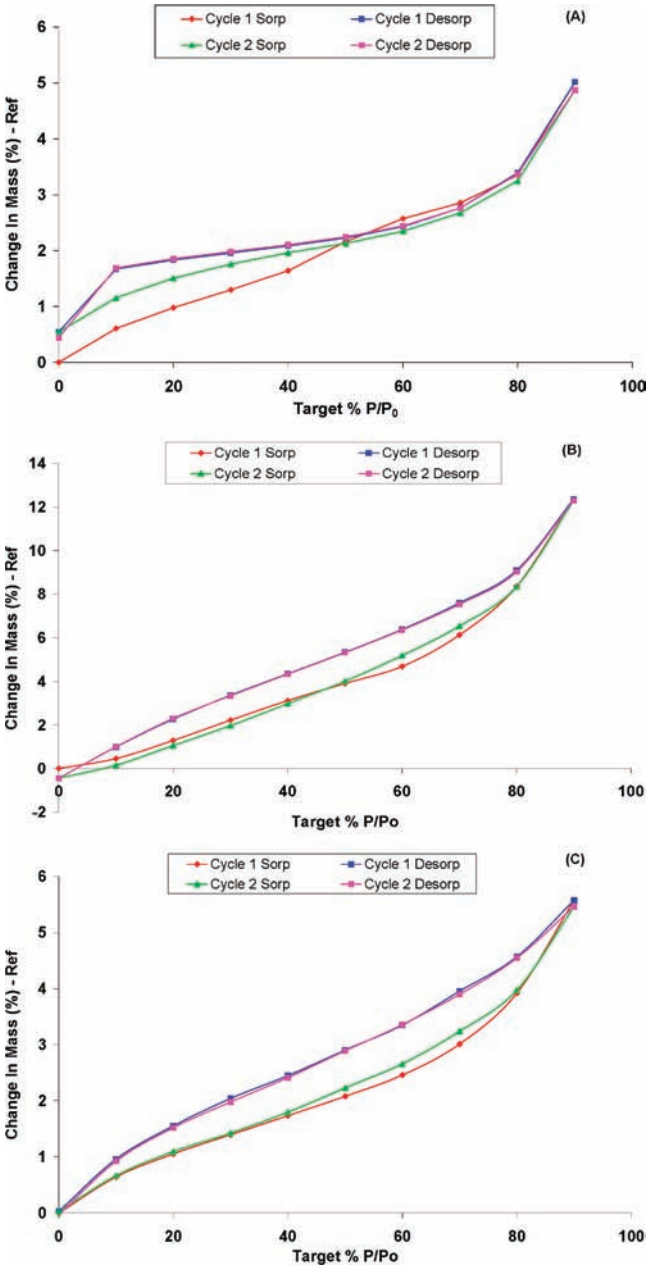

Figure 2. Water vapor sorption/desorption isotherms from two successive cycles for TRE-G (**A**), Pesta (**B**), and PEC-G (**C**) at 25 °C showing hysteresis.

formulations are quite different. The water uptake capacity obeys the trend TRE-G < PEC-G < Pesta. The differences are most drastic at 90% RH, at which TRE-G shows a 5.0% change in mass, PEC-G a 5.6% change in mass, and Pesta a 12.7% change in mass (**Figure 2**).

Together, the water uptake capacity and hysteresis results suggest that Pesta has the greatest capacity for bulk water absorption, followed by PEC-G and TRE-G. At present, it is unknown whether solid-state formulations exhibiting relatively poor water uptake capacity would be less efficacious biopesticides than those featuring greater uptake capacities. Further studies are required to confirm the significance of water uptake capacity as a useful property for improving the efficacy of solid-state biopesticide formulations and to determine whether water uptake capacity influences survival and germination of biopesticide propagules.

Water−Biopesticide Interactions. Large differences in the water sorption behavior among the three formulations are also evident.

Table 1. Difference between Sorption and Desorption Isotherms or Hysteresis for TRE-G, Pesta, and PEC-G at 25 °C

	difference in moisture content (%)		
RH (%)	TRE-G	Pesta	PEC-G
	Cycle I		
0.0	0.55	−0.45	0.03
10.0	1.06	0.54	0.32
20.0	0.85	0.98	0.50
30.0	0.66	1.14	0.65
40.0	0.44	1.23	0.71
50.0	0.07	1.42	0.82
60.0	−0.14	1.69	0.89
70.0	−0.09	1.47	0.94
80.0	0.04	0.74	0.65
90.0	0.00	0.00	0.00
	Cycle II		
0.0	−0.10	0.00	−0.05
10.0	0.54	0.85	0.26
20.0	0.35	1.24	0.43
30.0	0.22	1.37	0.55
40.0	0.14	1.35	0.62
50.0	0.12	1.31	0.66
60.0	0.10	1.17	0.70
70.0	0.09	1.00	0.66
80.0	0.12	0.68	0.57
90.0	0.00	0.00	0.00

TRE-G shows the biggest difference, with an apparent moisture-induced, irreversible change (**Figure 3A**). During the 60% RH sorption step, the mass initially increases and begins to steadily decrease instead of leveling off. This trend continues for the 70 and 80% RH steps. This decrease could be due to several reasons: release of volatile components, phase change, formulation degradation, or chemical reaction. Although there are several reasons, the liberation of volatile compounds, chemical reactions, and formulation degradation are unlikely explanations for the observed sorption behavior. The organic constituent materials in the TRE-G formulation, a high molecular weight carbohydrate (sodium carboxymethylcellulose) and a relatively low molecular weight sugar dimer (trehalose), are nonvolatile materials with very low or nearly zero vapor pressure and are chemically inert with respect to intraformulation ingredients under the prevailing experimental conditions. A more plausible explanation is that carbohydrates out of thermodynamic equilibrium, that is, trapped in metastable energy state(s), underwent a moisture-induced "phase" transition. In particular, trehalose is likely to be the material that would produce this change. A multipurpose additive in biopesticide formulations, trehalose is known to respond to increasing water activity by undergoing a second-order phase transition from an amorphous, metastable state lacking long-range order to a more ordered or crystalline state (*32*). The mass loss and the relatively longer durations necessary for mass equilibration between 60 and 80% RH are consistent with such a process (**Figure 3A**). With increasing moisture uptake, solute mobility increases, which facilitates crystallization (*33*). As the crystallization mechanism proceeds, "bound" water becomes "free" as it is expelled from the trehalose crystal lattice. In turn, the sample mass steadily decreases as expelled water molecules evaporate until dynamic equilibrium is reached between adsorbing and desorbing molecules, at which point no further change in mass is detectable.

Although it is unclear from these studies whether the anomaly observed is caused entirely by phase transitions of trehalose, the

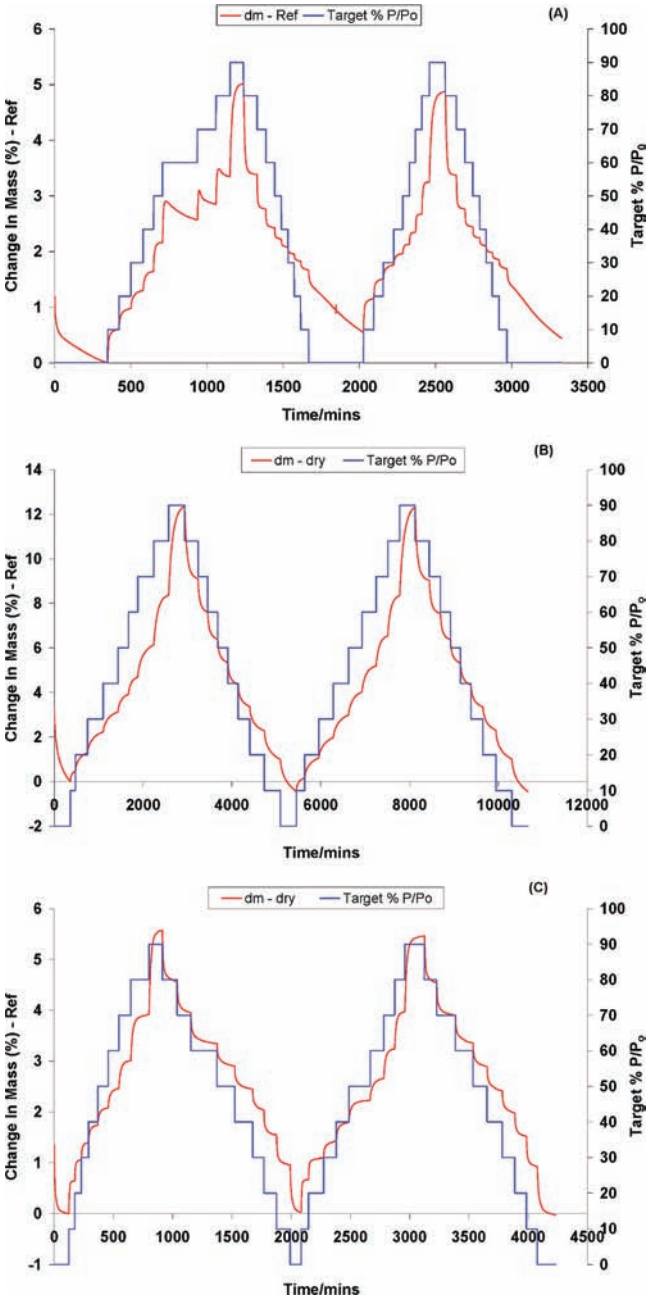

Figure 3. Two successive sorption/desorption cycles showing water sorption kinetics for TRE-G (**A**), Pesta (**B**), and PEC-G (**C**) at 25 °C.

observation is consistent with previous findings. In similar sorption analysis studies, Burnett et al. (*34*) reported on water sorption mediated crystallization of lactose, which was accompanied by a sharp loss in mass after crystallization. Other researchers have also reported on similar phenomenon, that is, the release and loss of water upon crystallization (*25*, *35*). The sorbed water vapor is most likely penetrating the bulk of the material, inducing this presumed phase change.

Interestingly, after the desorption process of cycle 1, the TRE-G sample did not return to its initial mass at 0% RH (**Figure 3A**). This indicates water mass uptake and further supports, in conjunction with mass conservation laws, the rejection of loss of volatiles and decomposition as plausible explanations for the anomaly in the sorption step. Whereas this uptake could be the result of chemical bond formation, it is likely instead to be in the form of physisorbed water onto trehalose monomers connected by hydrogen bonds or as hydrated crystals. The existence of trehalose in either an anhydrous or hydrated state is well-known (*35*−*37*) and so is the difference in sorption potential of the different crystalline forms (*32*). The transformation appears to be irreversible as the steady decreases in mass seen in the first cycle are not seen in the second sorption cycle (**Figure 3A**). Below the 60% RH level the second sorption isotherm is drastically different from the first cycle. A recent study evaluating the effects of aging on the physical properties of amorphous trehalose under experimental conditions similar to those presented concluded that water sorption could lead to irreversible changes in amorphous trehalose (*38*). Surana et al. also concluded that water sorption rate and potential were affected by nucleation. Similar results are observed for TRE-G and are discussed below. The implications of irreversible phase transitions in relation to efficacy of solid-state biopesticides are presently unknown.

Water Sorption Kinetics. Figure 3 displays the response times for equilibration as defined herein for TRE-G (**Figure 3A**), Pesta (**Figure 3B**), and PEC-G (**Figure 3C**) in response to positive and negative changes in the relative humidity of the surrounding air at 25 °C. The red trace, plotted on the left *y*-axis, indicates the percentage change in mass referenced to the dry mass (after initial drying stage), M_0, as a function of time. The blue trace, plotted on the right *y*-axis, traces the target percent partial pressure of water vapor or target relative humidity (see eq **1**) in the DVS as a function of time.

All three formulations show different response times. In the initial sorption cycle, PEC-G shows the fastest overall response to positive changes in relative humidity, followed by TRE-G and then Pesta. However, after the first rehydration/dehydration cycle, a different trend was observed. TRE-G emerged as the fastest formulation followed by PEC-G and then Pesta. In cycle 1, the response times for TRE-G and PEC-G to change A_w from 0.00 to 0.90 were 63 and 68% faster than Pesta, respectively, whereas in the subsequent cycle the response time was 78% (TRE-G) and 58% (PEC-G) faster than for Pesta, respectively. Evidently, the irreversible physicochemical change that occurred for TRE-G in cycle 1 affected the subsequent sorption behavior. The sorption kinetics of TRE-G stored at low A_w (<0.60) and then exposed to air with a high moisture content ($\geq$60% RH) is notably faster in cycle 2 than in cycle 1. After the physicochemical change, TRE-G sorbed water at a relatively faster rate than PEC-G and Pesta. The subsequent water uptake capacity of TRE-G was also affected by the physicochemical change. The moisture-induced physicochemical change to TRE-G decreased the formulation water uptake capacity by 11% or to ~4.5%. Similar results for trehalose have been reported (*38*).

Whereas the formulation response time to positive relative humidity changes > 10% obey one of the trends TRE-G (fastest) < PEC-G < Pesta (cycle 1) or PEC-G (fastest) < TRE-G < Pesta (cycle 2), the response time to decreases in relative humidty obeys the order TRE-G (fastest) < PEC-G < Pesta (slowest) for both cycles 1 and 2. The response time to negative changes in relative humidity are also different from the rehydration process for each formulation. In cycle 1, 71 and 57% faster response times with respect to Pesta were observed, respectively, for TRE-G and PEC-G in response to a change in relative humidity from 90 to 0.00%. A similar response was observed in cycle 2 for TRE-G (70%) and PEC-G (56%) (**Figure 3**). When the moisture level of air decreased from 90 to 0.00% RH, Pesta was slower than TRE-G and PEC-G by a factor of 3.4 and 2.3, respectively.

Fast sorption times for solid-state biopesticides could potentially lessen the dependency on long dew periods. Previous studies have established a correlation between dew periods and efficacy (*3*, *5*, *6*). One mechanism to improve efficacy might be to design biopesticides with short sorption times. After all three

Table 2. Correlation Coefficients (r) and Parameter Values Estimated from the GAB and Y&N Models for PEC-G, TRE-G, and Pesta at 25 °C[a]

formulation	C_{GAB}	K_{GAB}	monolayer capacity (mol/g)	r_{GAB}	$A_{Y\&N}$ (mol/g)	$B_{Y\&N}$ (mol/g)	$E_{Y\&N}$	$r_{Y\&N}$
				Cycle I				
PEC-G	0.801	7.76	0.000821	0.990	0.000452	0.001168	0.3210	0.995
TRE-G	0.762	6.49	0.000871	0.833	0.000569	0.000432	0.0660	0.986
Pesta					0.000719	0.003170	0.8570	0.966
				Cycle II				
PEC-G	0.779	6.925	0.000911	0.991	0.000511	0.000965	0.2860	0.998
TRE-G	0.791	293.8	0.000707	0.954	0.000667	0.000177	0.0037	0.990
Pesta					0.000719	0.003206	0.8570	0.997

[a] Fitted parameters C_{GAB}, K_{GAB}, and monolayer capacity (mol/g), W_M, are the three characteristic sorption properties of the sample according to the GAB model that is valid for $K_{GAB} \leq 1$. The parameters $A_{Y\&N}$, $B_{Y\&N}$, and $E_{Y\&N}$ are the Young and Nelson fit parameters, where $A_{Y\&N}$ is related to the amount of condensate adsorbed on the formulation sample surface, $B_{Y\&N}$ is the amount of condensate absorbed in the bulk, and $E_{Y\&N}$ is related to the binding strength of sorbed water vapor to the formulation surface. Values are obtained from analysis and fitting of the moisture sorption and desorption isotherm.

formulations were hydrated to a water activity of 0.90, Pesta, PEC-G, and TRE-G appear to be capable of producing up to 9, 4, and 2 h of sufficient "free" moisture, respectively, to a fungal biopesticide active if the air humidity decreased to <70% RH (**Figure 3**). The implication of this finding is that another mechanism to improve efficacy would be to engineer biopesticides with slow moisture desorption times. Such a formulation could effectively lengthen the duration in which "free" moisture is available for microbial activity despite decreases in ambient relative humidity.

Modeling of Sorption Isotherms. *GAB Model.* The GAB equation (eq **2**) was applied to the moisture sorption isotherms for TRE-G, Pesta, and PEC-G at 25 °C. For the PEC-G formulation, there was good correlation with the GAB model ($r \sim 0.990$). Neither Pesta (no fit) nor TRE-G in cycle 1 ($r = 0.833$) showed very good correlation with the GAB model. The W_m (mol/g), C, and K GAB parameter values (eq **2**) and correlation coefficients for cycles 1 and 2 are given in **Table 2**. Although the model is applicable over a wide range of A_w up to the maximum studied (0.90), the GAB equation did not provide a successful fit to the Pesta data, suggesting that the model is inappropriate for this formulation. This could be attributed to one or a combination of several factors. One factor may be the presence of non-equilibrium relative humidity steps in the isotherm. Another may be assumptions associated with the GAB model that are not applicable to these systems (i.e., the GAB model assumes homogeneous surface and monolayer formation). Experimental sorption properties had indicated the presence of a bulk absorption mechanism for all three formulations. Because the GAB model does not account for bulk absorption, this may be due to differences between the actual sorption mechanism and that proposed by the GAB model. Although the model shows relatively good fits to TRE-G ($r = 0.833$, cycle 1; $r = 0.954$, cycle 2) and PEC-G ($r = 0.990$, cycle 1; $r = 0.991$, cycle 2), the moisture uptake capacity for these two formulations was approximately 50% less than that of Pesta. The relatively stronger deviation in sorption mechanism between experiment and theory for Pesta may give rise to the lack of fit discovered when the GAB model was applied.

Although Pesta sorbed the most water, TRE-G and PEC-G also gained an appreciable amount of moisture (**Figure 2**). The disparity between the fittings of the GAB model to the different formulations suggests that the GAB model is not suitable for either PEC-G or TRE-G despite the good data fits. This conclusion is supported by the magnitude of the K_{GAB} values (**Table 2**) that exceed the limit $0 < K \leq 1$ imposed by the physics behind the GAB equations (*17*, *39*). The simplicity of this multilayer adsorption model is inadequate in describing the sorption behavior of these three biopesticide formulations.

Y&N Model. The Young and Nelson model showed good correlation with the experimental sorption isotherm data for all three formulations at 25 °C: TRE-G ($r = 0.986$, cycle 1; $r = 0.990$, cycle 2), Pesta ($r = 0.966$, cycle 1; $r = 0.997$, cycle 2), and PEC-G ($r = 0.995$, cycle 1; $r = 0.998$, cycle 2). The first cycle fits for TRE-G and Pesta show slightly lower r values when compared to PEC-G. This is most likely due to equilibrium not being reached at all relative humidity steps. Improved fitting may be achieved if all isotherm points were at equilibrium. However, because the r values for these samples are 0.96 or above, valid conclusions can be inferred from the fit parameters.

The A (eq **5**), B (eq **6**), and E (eq **10**) Y&N parameter values and correlation coefficients for cycles 1 and 2 are given in **Table 2**. In contrast to the GAB model, the Y&N model includes a hypothesis to account for the possibility of water being absorbed into the sample (*23*, *24*). Experimentally determined water uptake capacity and degree of hysteresis suggest the presence of a bulk absorption mechanism in the moisture sorption processes for all three formulations. The extra component in the Y&N model may explain the relatively better correlation coefficient values in comparison to the GAB model. As a result, the Y&N model is able to provide additional insight into the distribution of water sorbed by the three biopesticide formulations.

$E_{Y\&N}$ is an energy term relating to the strength of interaction of water vapor with the surface of the sample (eq **10**) and is similar to the C term in the GAB model. The $A_{Y\&N}$ term is related to the moisture capacity of a monomolecular layer (eq **5**) and is similar to W_m in the GAB model, whereas $B_{Y\&N}$ is related to the amount of moisture absorbed by the sample and has no counterpart in the GAB model (eq **6**). After experimental data are fitted and the A, B, and E terms are obtained, the remaining parameters θ, α, and φ can be calculated using eqs **7**, **8**, and **9**, respectively. These parameters can then be used to determine the distribution of moisture for a sample at a particular A_w during a sorption or desorption cycle by using eqs **3** and **4**, respectively. **Table 3** presents the Y&N moisture distribution for TRE-G, Pesta, and PEC-G as each formulation undergoes a rehydration process from a dry state ($A_w = 0$). Also shown is the equilibrium moisture content of each of the three formulations at each relative humidity. $A\theta$ is the amount of moisture present in the first monolayer, $A(\theta + \alpha)$ is the amount of moisture externally adsorbed and includes the first molecular monolayer plus the so-called "multilayer", and $B\varphi$ is the amount of moisture internally absorbed or "bulk" moisture (*26*). The amount of moisture is expressed as a percentage of the moisture content at each relative humidity. **Table 4** summarizes the moisture distribution of TRE-G, Pesta, and PEC-G at 25 °C and at each relative humidity investigated during the desorption process.

Table 3. Comparison of TRE-G, Pesta, and PEC-G Sorption Moisture Distribution for Successive Sorption Cycles at 25 °C According to the Y&N Model[a]

	TRE-G				Pesta				PEC-G			
RH (%)	sorption moisture content (% w/w)	$A\theta$	$A(\theta+\alpha)$	$B\varphi$	sorption moisture content (% w/w)	$A\theta$	$A(\theta+\alpha)$	$B\varphi$	sorption moisture content (% w/w)	$A\theta$	$A(\theta+\alpha)$	$B\varphi$
					Cycle I							
0.0	0.00	0	0	0	0.00	0.00	0.00	0.00	0.00	0.0	0.0	0.0
10.0	0.61	84.6	93.6	6.4	0.45	64.6	71.5	28.5	0.64	73.2	81.1	18.9
20.0	0.98	72.5	89.0	11.0	1.29	47.3	58.3	41.7	1.05	57.2	70.4	29.6
30.0	1.30	62.8	85.7	14.3	2.22	37.0	51.0	49.0	1.39	46.6	63.9	36.1
40.0	1.64	54.8	83.4	16.6	3.12	30.2	46.8	53.2	1.73	38.8	59.9	40.1
50.0	2.16	47.8	81.8	18.2	3.91	25.2	44.5	55.5	2.08	32.9	57.4	42.6
60.0	2.57	41.7	81.0	19.0	4.69	21.3	43.6	56.4	2.46	28.2	56.3	43.7
70.0	2.85	36.1	80.8	19.2	6.13	18.1	44.0	56.0	3.01	24.2	56.3	43.7
80.0	3.35	30.5	81.4	18.6	8.36	15.3	45.9	54.1	3.92	20.5	57.6	42.4
90.0	5.02	24.5	83.2	16.8	12.35	12.5	50.4	49.6	5.57	16.7	61.2	38.8
					Cycle II							
0.0	0.00	0	0	0	0.00	0.00	0.00	0.00	0.00	0.0	0.0	0.0
10.0	0.60	88.3	97.7	2.3	0.60	64.4	71.3	28.7	0.63	77.2	85.4	14.6
20.0	0.96	78.3	95.8	4.2	1.50	47.1	58.0	42.0	1.06	62.2	76.5	23.5
30.0	1.21	69.6	94.5	5.5	2.42	36.8	50.7	49.3	1.39	51.6	70.8	29.2
40.0	1.41	61.8	93.4	6.6	3.43	30.0	46.5	53.5	1.76	43.6	67.1	32.9
50.0	1.58	54.7	92.7	7.3	4.46	25.0	44.2	55.8	2.20	37.2	64.8	35.2
60.0	1.80	48.1	92.3	7.7	5.63	21.2	43.3	56.7	2.63	32.0	63.7	36.3
70.0	2.13	41.8	92.2	7.8	6.98	18.0	43.7	56.3	3.21	27.4	63.7	36.3
80.0	2.70	35.4	92.5	7.5	8.80	15.2	45.6	54.4	3.94	23.2	64.9	35.1
90.0	4.33	28.2	93.3	6.7	12.74	12.4	50.2	49.8	5.43	18.8	68.1	31.9

[a] $A\theta$ is the amount of moisture in the first molecular layer, $A(\theta+\alpha)$ is the amount of moisture externally adsorbed and includes the first molecular monolayer, and $B\varphi$ is the amount of moisture internally absorbed. Amounts are expressed as a percentage of the moisture content.

Table 4. Comparison of TRE-G, Pesta, and PEC-G Sorption Moisture Distribution for Successive Desorption Cycles at 25 °C According to the Y&N Model[a]

	TRE-G				Pesta				PEC-G			
RH (%)	desorption moisture content (% w/w)	$A\theta$	$A(\theta+\alpha)$	$B\varphi$	desorption moisture content (% w/w)	$A\theta$	$A(\theta+\alpha)$	$B\varphi$	desorption moisture content (% w/w)	$A\theta$	$A(\theta+\alpha)$	$B\varphi$
					Cycle I							
0.0	0.00	0.0	0.0	0.0	0.00	0.0	0.0	0.0	0.00	0.0	0.0	0.0
10.0	1.12	55.9	61.8	38.2	1.44	19.7	21.8	78.2	0.93	29.1	32.2	67.8
20.0	1.28	52.4	64.2	35.8	2.72	19.2	23.7	76.3	1.52	28.1	34.6	65.4
30.0	1.41	48.8	66.6	33.4	3.81	18.7	25.8	74.2	2.01	27.0	37.1	62.9
40.0	1.53	45.3	69.0	31.0	4.80	18.1	28.1	71.9	2.42	25.9	39.9	60.1
50.0	1.68	41.8	71.5	28.5	5.78	17.4	30.8	69.2	2.87	24.6	42.9	57.1
60.0	1.88	38.1	74.0	26.0	6.83	16.6	34.0	66.0	3.32	23.1	46.2	53.8
70.0	2.22	34.2	76.6	23.4	8.05	15.6	37.9	62.1	3.92	21.5	50.1	49.9
80.0	2.84	29.9	79.6	20.4	9.54	14.4	43.0	57.0	4.54	19.5	54.7	45.3
90.0	4.47	24.5	83.2	16.8	12.80	12.5	50.4	49.6	5.54	16.7	61.2	38.8
					Cycle II							
0.0	0.00	0.0	0.0	0.0	0.00	0.0	0.0	0.0	0.00	0.0	0.0	0.0
10.0	1.25	74.4	82.2	17.8	1.45	19.5	21.6	78.4	0.95	35.6	39.4	60.6
20.0	1.42	68.4	83.7	16.3	2.75	19.1	23.5	76.5	1.55	34.1	42.0	58.0
30.0	1.54	62.7	85.0	15.0	3.79	18.6	25.6	74.4	2.01	32.6	44.7	55.3
40.0	1.66	57.1	86.4	13.6	4.78	18.0	27.9	72.1	2.44	30.9	47.5	52.5
50.0	1.81	51.7	87.6	12.4	5.77	17.3	30.6	69.4	2.92	29.1	50.6	49.4
60.0	2.00	46.4	88.9	11.1	6.81	16.5	33.8	66.2	3.39	27.1	54.0	46.0
70.0	2.32	40.9	90.2	9.8	7.98	15.5	37.7	62.3	3.92	24.9	57.7	42.3
80.0	2.93	35.1	91.6	8.4	9.47	14.3	42.7	57.3	4.57	22.2	62.2	37.8
90.0	4.44	28.2	93.3	6.7	12.74	12.4	50.2	49.8	5.49	18.8	68.1	31.9

[a] $A\theta$ is the amount of moisture in the first molecular layer, $A(\theta+\alpha)$ is the amount of moisture externally adsorbed and includes the first molecular monolayer, and $B\varphi$ is the amount of moisture internally absorbed. Amounts are expressed as a percentage of the moisture content.

As can be seen from **Table 3**, the relative distribution of moisture in the three different locations—monolayer, multilayer, and bulk—are quite different among the three formulations. For example, **Table 3** shows Pesta exhibits the greatest capacity for bulk water followed by PEC-G and then TRE-G. This trend is evidently independent of cycle effects. These results are consistent

with the experimentally determined uptake capacity. An identical trend was observed for the uptake capacity. Another trend observable in **Table 3** is the amount of moisture in the first molecular layer in direct contact with the sample surface. Although there is no simple experiment to experimentally confirm the amount of moisture at the water-surface interface, the Y&N model indicates that TRE-G has the greatest capacity to hold water at this interface, followed by PEC-G and Pesta.

Table 4 presents the Y&N moisture distribution for each formulation as the materials undergo a dehydration process starting from a "wet" state ($A_w = 0.90$). It can be seen that the majority of the water content of Pesta is distributed within the bulk, followed by PEC-G and then TRE-G. This trend is independent of cycle effects. These results are consistent with the experimentally observed response times for the formulation in response to negative changes in relative humidity.

Optimal Water Activity. TRE-G and PEC-G are newly developed formulations that have been used as microbial delivery systems for other applications (*27*). Very little is known about the shelf life of various microorganisms in either PEC-G or TRE-G, in contrast to Pesta. Several researchers have shown that shelf life, in terms of microbial viability, is optimal when Pesta is dried and stored at low water activities. Connick et al. (*11*) demonstrated that *C. truncatum* viability is best in Pesta stored at 0, 12, or 33% RH in comparison to 53 and 75% RH. Honeycutt and Benson (*40*) reported on enhanced binucleate *Rhizoctonia* spp. survival in Pesta stored at 12 or 33% RH by approximately 2−3 months in comparison to 53 and 75% RH. Shabana et al. (*14*) reported optimal shelf life at 11% RH for *Fusarium oxysporum* f. sp. *orthoceras* in contrast to 53 and 59% RH. In all of these shelf-life studies, a similar storage temperature of 25 °C was used. Although low water activity may be conducive to long shelf life, a practical solid-state biopesticide must be able to hydrate from the dry state to an appreciable moisture level within a probable duration in which high moisture levels are present to facilitate microbial growth and infection. For fungal growth, an $A_w \geq 0.70$ is generally required, whereas a higher A_w exceeding 0.89 is typically required for bacterial growth (*4*), making irrigated crop systems or long dew periods ideal conditions for biopesticides. To cause severe infection of target weeds, a minimum dew period of 12 h is required (*3*). For biopesticides to be considered as a competitive pest control tool, they must be able to perform in the absence of a dew period and/or with dew periods of <12 h, which is more likely to occur than the presence of dew periods of >12 h. Whereas Pesta shows the greatest capacity to gain water, it shows the slowest response to changes in relative humidity. For example, Pesta initially at $A_w = 0.10$ needed at least 4.5 h to reach a water activity of 0.20 when the ambient air changed to 20% RH. By comparison, TRE-G and PEC-G required comparatively less time, 1.3 and 0.9 h, respectively (**Figure 3**). It is interesting to note that Pesta dried to a $A_w = 0.10$ would require 29−41 h to reach a water activity of 0.70−0.90 or to facilitate bacterial/fungal growth, whereas TRE-G and PEC-G would require a minimum of approximately 8.6 and 7.9 h, respectively, to enable fungal growth or 13.6 and 12.3 h, respectively, to facilitate bacterial growth. As indicated earlier, one mechanism to improve efficacy might be to design biopesticides with fast sorption rates.

New Paradigm. The ability to identify, measure, and optimize properties that correlate to stability or efficacy will be crucial for the success of future biopesticides. Although no organism was incorporated into TRE-G, Pesta, or PEC-G, the DVS method of analysis proved to be useful in the comparison of these different matrices. Despite TRE-G and PEC-G sharing a similar component, Satintone 5HB, at a concentration $>75\%$, the formulations could still be differentiated by several sorption properties. Thus, sorption properties can be monitored using the dynamic vapor sorption technique and may be used as guides in the designing and tailoring of formulations. These initial studies suggest that advancements in biopesticide development in regard to water−biopesticide interactions may be possible through the use of a dynamic vapor sorption analyzer.

Similar to other industries such as drugs, pharmaceuticals, and cosmetics, the active materials for microbial biopesticides are often dependent on a carrier for chemical and physical stability and to improve bioavailability. All ingredients in a formulation including the active material contribute to the sorption behavior of the product (*41*). However, sorption studies on carrier matrices devoid of the active ingredient are frequently performed to compare different constituent materials and candidate formulations (*42*,*43*). Although an effect on sorption properties may arise from addition of an active material, the contribution is largely consistent across carrier matrices because the chemical potential μ and activity a of the active ingredient remain unchanged (*44*). Thus, the desired sorption behavior is governed by the carrier matrix components and composition. Consequently, emphasis may be directed towards identifying functional matrices. However, unlike neat chemical actives, the contribution by a microbial active will be intrinsic not only to the organism of interest but also to any associated residual chemistries from the particular methods of cultivation and harvesting. In other words, the microbial contribution to the sorption behavior of potential biopesticide matrices is the same regardless of carrier matrix for a given source of the microbial active.

Earlier shelf-life studies that used saturated solutions were limited to discrete relative humidity values attainable with common salts. Consequently, it remains unclear whether formulations stored at water activities between 0.33 and 0.53 would exhibit shelf life comparable to those stored at 0, 0.12, and 0.33. Because the need to lessen the dependency on lengthy dew periods has been a long-standing challenge in biopesticide development, new approaches may be necessary. **Figure 3** illustrates that Pesta stored at $A_w = 0.40$ would require about 60% less time to rehydrate to a $A_w = 0.70$ in contrast to storage at $A_w = 0.10$. TRE-G and PEC-G would require ∼65 and 61% less time, respectively. A significant implication of these findings is that both the storage− and infection−moisture requirements should be considered simultaneously when a final storage water activity is selected for solid-state biopesticides.

The findings suggest that a dew period may not be imperative for solid-state formulations; however, a sufficiently high humidity would be required. Furthermore, the data shown in **Figure 3** indicate that a sufficiently long exposure to highly humid air would also be required. The minimum exposure duration to support microbial growth is shown to be influenced by formulation. It has also been shown that sorption (hydration) and desorption (dehydration) kinetics are potentially important properties that should be considered in the development and optimization of biopesticides. The ideal solid-state biopesticide would exhibit fast hydration kinetics and a slow dehydration rate. Optimization of such a biopesticide would involve optimizing sorption and desorption kinetics of the carrier matrix in addition to other properties that may be required, such as UV resistance or rainfastness.

In summary, water vapor sorption experiments were performed on three different biopesticide formulations. The formulations could be differentiated by sorption properties, that is, water uptake capacity and rehydration/dehydration rates. The experimental

results indicate a bulk absorption dominated moisture-sorption mechanism for all three formulations. The in situ video images did not reveal any visible transformations, except for minor swelling. It was found that the GAB model is not appropriate for these formulations. The Y&N model showed good correlation with experimental data. Of the three formulations, Pesta shows the greatest moisture uptake capacity followed by PEC-G and then TRE-G; however, Pesta was very slow to rehydrate. The response time order was PEC-G (fastest) < TRE-G < Pesta (slowest) for rehydration and TRE-G (fastest) < PEC-G < Pesta (slowest) for dehydration.

ACKNOWLEDGMENT

We thank Leon Hicks for technical support.

LITERATURE CITED

(1) Landcare Research. What's New in Biological Control of Weeds? Newsletter Issue 34, **2005**.

(2) Jones, K. A. Burges, H. G. Introduction. In *Formulation of Microbial Biopesticides, Beneficial Microorganisms, Nematodes and Seed Treatments*; Burges, H. D., Ed.; Kluwer Academic: London, U.K., 1998; pp 1−4.

(3) Auld, B. A.; Morin, L. Constraints in the development of bioherbicides. *Weed Technol*. **1995**, *9*, 638–652.

(4) Christian, J. H. B. Drying and reduction of water activity. In *The Microbiological Safety and Quality of Food*; Lund, B. M., Baird-Parker, T. C., Gould, G. W., Eds.; Springer: New York, 2000; Vol. I, pp 146−174.

(5) Auld, B. A.; McRae, C. F.; Say, M. M. Possible control of *Xanthium spinosium* by a fungus. *Agric. Ecosyst. Environ*. **1988**, *21*, 219–23.

(6) Boyette, C. D. Unrefined corn oil improves the mycoherbicidal activity of *Colletotrichum truncatum* for hemp sesbania (*Sesbania exaltata*) control. *Weed Technol*. **1994**, *8*, 526–529.

(7) Burges, H. G. Formulation of mycoinsecticides. In *Formulation of Microbial Biopesticides, Beneficial Microorganisms, Nematodes and Seed Treatments*; Burges, H. D., Ed.; Kluwer Academic: London, U.K., 1998; pp 131−185.

(8) Auld, B. A.; Hetherington, S. D.; Smith, H. E. Advances in bioherbicide formulation. *Weed Biol. Manag*. **2003**, *3*, 61–67.

(9) Connick, W. J., Jr.; Daigle, D. J.; Quimby, P. C., Jr. An improved invert emulsion with high water retention for mycoherbicides delivery. *Weed Techol*. **1991**, *5*, 442–444.

(10) Womack, J. G.; Eccleston, G. M.; Burge, M. N. A vegetable oil-based invert emulsion for mycoherbicides delivery. *Biol. Control* **1996**, *6*, 23–28.

(11) Connick, W. J., Jr.; Daigle, D. J.; Boyette, C. D.; Williams, K. S.; Vinyard, B. T.; Quimby, P. C., Jr. Water activity and other factors that affect the viability of *Colletotrichum truncatum* conidia in wheat Four-kaolin granules ('Pesta')'. *Biocontrol Sci. Technol*. **1996**, *6*, 277–284.

(12) Duan, W.; Yang, E.; Xiang, M.; Liu, X. Effect of storage conditions on the survival of two potential biocontrol agents of nematodes, the fungi *Paecilomyces lilacinus* and *Pochonia chlamydosporia*. *Biocontrol Sci. Technol*. **2008**, *18*, 613–620.

(13) Friesen, T. J.; Holloway, G.; Hill, G. A.; Pugsley, T. S. Effect of conditions and protectants on the survival of *Penicillium bilaiae* during storage. *Biocontrol Sci. Technol*. **2006**, *16*, 89–98.

(14) Shabana, Y. M.; Mueller-Stoever, D.; Sauerborn, J. Granular Pesta formulation of *Fusarium oxysporum* f. sp. *orthoceras* for biological control of sunflower broomrape: efficacy and shelf-life. *Biol. Control* **2003**, *26*, 189–201.

(15) Da Silva, R. Z.; Neves, P. M. J. O.; Yamashita, F.; Santoro, P. H. Water sorption isotherms of *Beauveria bassiana* (Bals.) Vuill. conidia. *Neotrop. Entomol*. **2003**, *32*, 347–350.

(16) Hong, T. D.; Edgington, S.; Ellis, R. H.; de Muro, M. A.; Moore, D. Saturated salt solutions for humidity control and the survival of dry powder and oil formulations of *Beauveria bassiana* conidia. *J. Invert. Pathol*. **2005**, *89*, 136–143.

(17) Blahovec, J.; Yanniotis, S. GAB generalized equation for sorption phenomena. *Food Bioprocess Technol*. **2008**, *1*, 82–90.

(18) Rahman, M. S. Glass transition and state diagram of foods. In *Handbook of Food Preservation*; Rahman, M. S., Ed.; CRC Press: Boca Raton, FL, 2007; pp 335−363.

(19) Chirife, J.; Iglesias, H. A. Equations for fitting water sorption isotherms of foods: part 1 − a review. *J. Food Technol*. **1978**, *13*, 159–174.

(20) van den Berg, C.; Bruin, S. Water activity and its estimation in food systems. In *Water Activity: Influence on Food Quality*; Rockland, L. B., Stewart, F., Eds.; Academic Press: New York, 1981; pp 147−177.

(21) de Boer, J. H. *The Dynamical Character of Adsorption*, 2nd ed.; Clarendon Press: Oxford, U.K., 1968; pp 200−219.

(22) Brunauer, S.; Emmett, P. H.; Teller, E. Adsorption of gases in multimolecular layers. *J. Am. Chem. Soc*. **1938**, *60*, 309–319.

(23) Young, J. H.; Nelson, G. L. Theory and hysteresis between sorption and desorption isotherms in biological materials. *Trans. Am. Soc. Agric. Eng*. **1967**, *10*, 260–263.

(24) Young, J. H.; Nelson, G. L. Research and hysteresis between sorption and desorption isotherms of wheat. *Trans. Am. Soc. Agric. Eng*. **1967**, *10*, 756–761.

(25) Buckton, G.; Darcy, P. The use of gravimetric studies to assess the degree of crystallinity of predominantly crystalline powders. *Int. J. Pharm*. **1995**, *123*, 265–271.

(26) Nokhodchi, A.; Ford, J. L.; Rubinstein, M. H. Studies on the interaction between water and (hydropropyl) methylcellulose. *J. Pharm. Sci*. **1997**, *86*, 608–615.

(27) Lyn, M. E.; Abbas, H. K.; Zablotowicz, R. M.; Johnson, B. J. Delivery systems for biological control agents to manage aflatoxin contamination of pre-harvest maize. *Food Addit. Contam*. **2009**, *26*, 381–387.

(28) Daigle, D. J.; Connick, W. J., Jr.; Boyette, C. D.; Lovisa, M. P.; Williams, K. S.; Watson, M. Twin-screw extrusion 'Pesta'-encapsulated biocontrol agents. *World J. Microbiol. Biotechnol*. **1997**, *13*, 671–676.

(29) Wolf, W.; Spiess, W. E. L.; Jung, G. Standardization of isotherm measurements. In *Properties of Water in Foods in Relation to Food Quality and Stability*; Simatos, D., Multon, J. L., Eds.; Martinus Nijhoff Publishers: Dordrecht, The Netherlands, 1985; pp 661−679.

(30) van Aken, G. A. Polysaccharides in food emulsions. In *Food Polysaccharides and Their Applications*; Stephen, A. M., Phillips, G. O., Williams, P. A., Eds.; CRC Press: Boca Raton, FL, 2006; pp 521−539.

(31) Rahman, M. S.; Labuza, T. P. Water activity and food preservation. In *Handbook of Food Preservation*; Rahman, M. S., Ed.; CRC Press: Boca Raton, FL, 2007; pp 447−476.

(32) Iglesias, H. A.; Chirife, J.; Buera, M. P. Adsorption isotherm of amorphous trehalose. *J. Sci. Food Agric*. **1997**, *75*, 183–186.

(33) Roos, Y. H. Glass transition-related physiochemical changes in foods. *Food Technol*. **1995**, *10*, 97–102.

(34) Burnett, D. J.; Thielmann, F.; Booth, J. Determining the critical relative humidity for moisture-induced phase transitions. *Int. J. Pharm*. **2004**, *287*, 123–133.

(35) Iglesias, H. A.; Chirife, J. Delayed crystallization of amorphous sucrose in humidified freeze dried model systems. *J. Food Technol*. **1978**, *13*, 137–144.

(36) Sussich, F.; Urbani, R.; Princivalle, F.; Cesaro, A. Polymorphic amorphous and crystalline forms of trehalose. *J. Am. Chem. Soc*. **1998**, *120*, 7893–7899.

(37) Taylor, L. S.; York, P. Effect of particle size and temperature on the dehydration kinetics of trehalose dehydrate. *J. Pharm. Sci*. **1998**, *167*, 215–221.

(38) Surana, R.; Pyne, A.; Suryanarayanan, R. Effect of aging on the physical properties of amorphous trehalose. *Pharm. Res*. **2004**, *21*, 867–874.

(39) Lewicki, P. P. The applicability of the GAB model to food water sorption isotherm. *Int. J. Food Sci. Technol*. **1997**, *31*, 553–557.

(40) Honeycutt, E. W.; Benson, D. M. Formulation of binucleate *Rhizoctonia* spp. and biocontrol of *Rhizoctonia solani* on impatiens. *Plant Dis*. **2001**, *85*, 1241–1248.

(41) Caurie, M. Water activity of multicomponent mixture of solutes and non-solutes. *Int. J. Food Sci. Technol.* **2005**, *40*, 295–303.
(42) Airaksinen, S.; Karjalainen, M.; Shevchenko, A.; Westermarck, S.; Leppanen, E.; Rantanen, J.; Yliruusi, J. Role of water in the physical stability of solid dosage formulations. *J. Pharm. Sci.* **2005**, *94*, 2147–2165.
(43) Li, Y.; Sanzgiri, Y. D.; Chen, Y. A study on moisture isotherms of formulations: the use of polynomial equations to predict the moisture isotherms of tablet products. *AAPS PharmSciTech* **2003**, *4*, 1–8.
(44) Mortimer, R. G. *Physical Chemistry*; Elsevier Academic Press: Burlington, MA, 2008; pp 267−270.

Received for review May 13, 2009. Revised manuscript received December 18, 2009. Accepted December 22, 2009. Mention of trade names or commercial products is solely for the purpose of providing specific information and does not imply recommendation or endorsement by the U.S. Department of Agriculture.